



# Traces of collisional and transtensional processes between the Carpathia and the European platform in the geoelectric image (NE Slovakia and SE Poland)

Vladimír Bezák<sup>1</sup> · Lenka Ondrášová<sup>1,4</sup> · Ján Vozár<sup>1</sup> · Szymon Oryński<sup>2</sup> · Jozef Madzin<sup>1</sup> · Dušan Majcin<sup>1</sup> · Radek Klanica<sup>3</sup> · Dušan Bilčík<sup>1</sup>

Received: 29 August 2023 / Accepted: 31 October 2023  
© The Author(s) 2024

## Abstract

We present the latest magnetotelluric models on profiles in the northeastern part of Slovakia and the southeastern part of Poland. These models are focused on deciphering the tectonic structures at the contact of the Inner Carpathians with the European Platform in this area. For the Inner Carpathian block, we propose the term Carpathia. Profile SA-01 shows shallower structures and the parallel MT-05 profile shows deeper structures. These models are also correlated with the seismic profile CEL-05. All results are compatible and show an original subduction-collisional structure, which was later replaced by a transpressive-transtensional one. The most striking structures are thick highly conductive subhorizontal zones in the middle crust and a tectonically controlled deep vertical conductive structure—the Carpathian conductive zone. Other significant structures, which also appear in the seismic section, are back thrusting of Flysch Belt and the Klippen Belt basement (Penninic crust) uplift.

**Keywords** Western Carpathians · Magnetotelluric sounding · Contact zone · Subduction · Collision

## Introduction

Most of the authors who created the models of Neoalpine tectonic development of the Carpatho–Pannonian region are based on the assumption of the subduction of the North Penninic Ocean, the gradual approach of the terranes from the Alps and their final collision with the European Platform

(e.g. Csontos et al. 1992; Konečný et al. 2002; Kováč et al. 1998, Froitzheim et al. 2008 and others, see the chapters dedicated to geology in these articles). Both subduction and collision progressed along the arc-shaped edge of the European Platform (EP) from W to E, terminating in the Eastern Carpathians (Vrancea).

The tectonic block of the Inner Western Carpathians (IWECA) belongs to the Neoalpine (Neogene) terranes, which were pushed out of the Alps area into the area of the North Penninic Ocean (in this case, the Magura flysch ocean). Owing to their simplicity and compatibility with the other terranes of the Pannonian area (Dacia, Tisia, Pelsonia), we propose the abbreviated name Carpathia (CA) for this block. Carpathia is composed of Paleozoic tectonic units (comprising older Hercynian crustal units and Upper Paleozoic and Mesozoic complexes) and remnants of Mesozoic tectonic units (mainly the Orava complexes of today's Klippen Belt and their basement–Penninic crust (PC)). During collision of CA with EP Flysch Belt of Outer Western Carpathians (OWECA) originated. In the north along all Carpathian arc, CA is bounded by EP along the tectonic shear zone demonstrated as the Carpathian Conductivity Zone (CCZ), which is connected with

---

Edited by Prof. Teresa Grabowska (ASSOCIATE EDITOR) / Prof. Ramón Zúñiga (CO-EDITOR-IN-CHIEF).

---

✉ Ján Vozár  
geofjavo@savba.sk

- <sup>1</sup> Earth Science Institute of the Slovak Academy of Sciences, Dúbravská cesta 9, 840 05 Bratislava, Slovak Republic
- <sup>2</sup> Institute of Geophysics, Polish Academy of Sciences, Księcia Janusza 64, 01-474 Warsaw, Poland
- <sup>3</sup> Institute of Geophysics, Academy of Sciences of the Czech Republic, Boční II/1401, 141 31 Prague 4, Czech Republic
- <sup>4</sup> Department of Engineering Geology, Hydrogeology and Applied Geophysics, Faculty of Natural Sciences, Comenius University, Mlynská Dolina, Ilkovičova 6, 842 48 Bratislava, Slovakia

the Carpathian Conductivity anomaly (CCA) and in the SW, S and SE, it interfaces with Pelsonia along the Rába–Hurbanovo–Diósjenő, eventually Darnó faults, in the west is bounded to the Eastern Alps block by system of Leitha–Lab faults (Fig. 1).

Using MT modelling on the profiles across the contact zone between Carpathia and the EP, we identified a different nature of collisional processes in the western and eastern parts of the Western Carpathian arc (Bezák et al. 2021). While the oblique collision style dominated in the western part, the direct collision style was dominant in the eastern part. This was also manifested by different tectonics inside the Carpathian block, which was divided into two sub-blocks along important shear zone (Pohorelá fault, possibly continuation of Rába fault).

The previous magnetotelluric (MT) measurements were located almost near the border of these sub-blocks (e.g. Majcin et al. 2018). For this reason, the aim of our subsequent studies was to verify the tectonic structures directly in the centre of the eastern sub-block. For this purpose, in cooperation with geophysicists from Polish Institute of Geophysics of PAS and Czech Institute of Geophysics CAS, we carried out MT measurements along the profile SA-01 that runs in the SW-NE direction perpendicular to the collision

zone in the NE part of Slovakia and the SE part of Poland (Figs. 1 and 2). On the surface, the profile intersects the units of the Inner Carpathian Paleogene (ICP), Klippen Belt (KB), and the units of the outer flysch (FB). In addition to determining the nature of the tectonic structures, the goal was also to verify the manifestations of CCZ in this area.

Information on shallower structures from the SA-01 profile is complemented by information on deeper structures from the parallel MT-05 profile following the CELEBRATION 2000 CEL-05 seismic profile (Figs. 1 and 2). The results of this seismic model CEL-05 (Janik et al. 2009, 2011) as well as the results of geothermal modelling (Majcin et al. 2014) were utilised in this study for geological and tectonic interpretation.

## Geology and tectonics

The Western Carpathians (WECA) form the northernmost segment of the Alpine–Carpathian orogenic loop and the westernmost northward convex branch of the Carpathian arc. After Tectonic map of Slovakia (Bezák et al. 2004) they can be divided into two main tectonic zones: Outer (OWECA)



**Fig. 1** Schematic map of the Carpatho–Pannonian region (after Majcin et al. 2018) with position of investigated area and profiles SA-01 and MT-05. Structure description: (1) European platforms, (2) Foredeep units, (3) Alpine–Outer Carpathian Flysch Belt, (4) Klippen Belt, (5) Inner Alpine–Carpathian units, (6) Neogene volcan-

ites on the surface, (7) Neogene sediments. EA—Eastern Alps. Blue lines—borders of Carpathia. Fault system: CCZ—Carpathian conductive zone, Li—Leitha-Láb, Rb—Rába, Ph—Pohorelá, Hu—Hurbanovo, Ds—Diósjenő

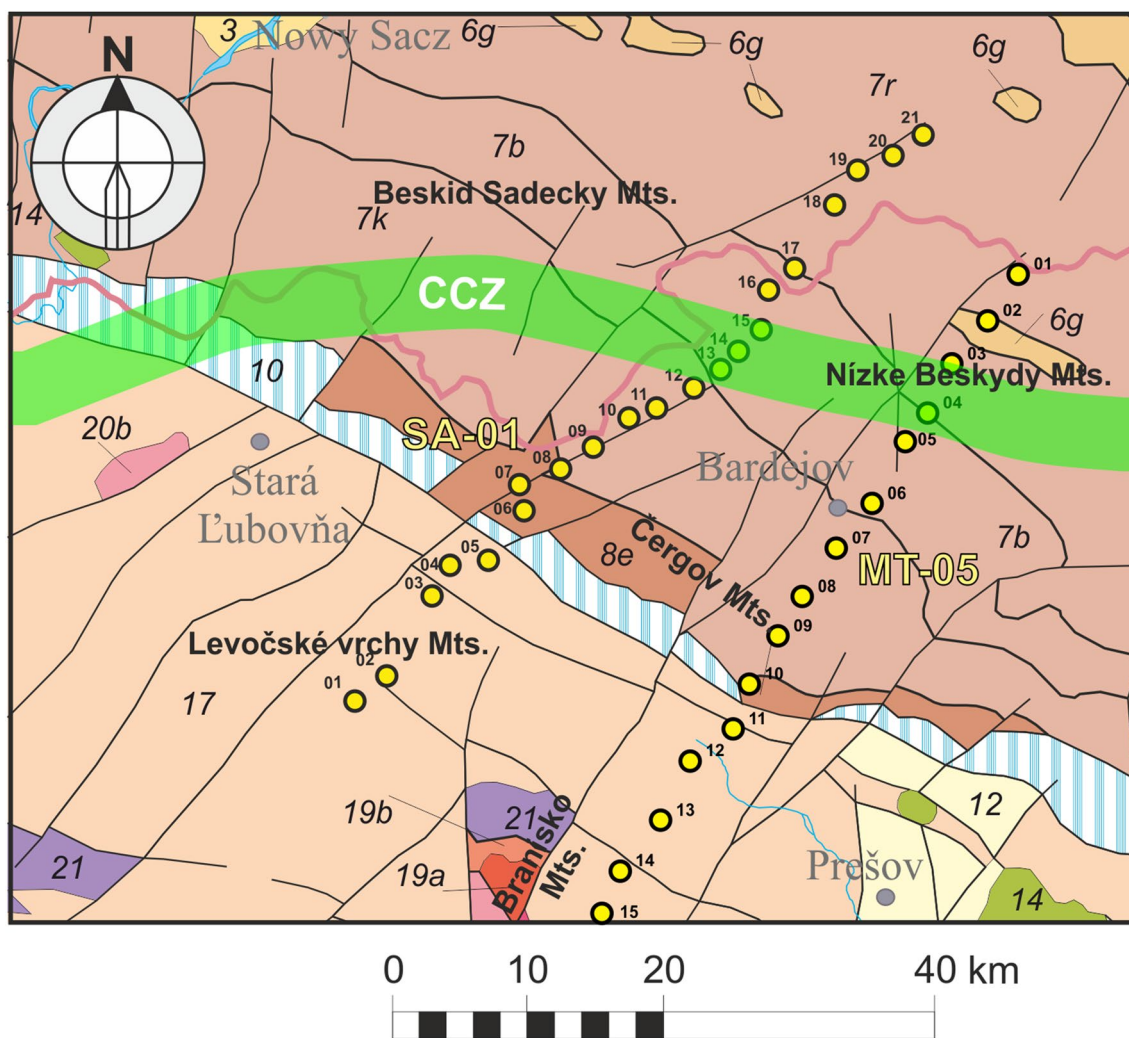


**Fig. 2** Tectonic scheme of investigated area after Lexa et al. (2000) and position of MT profiles. Yellow circles—positions of the measured MT sites. Green stripe—CCZ. 3—Units of folded molasse, 6—Foremagura unit of the Flysch Belt (g—Grybów fm.), 7—Magura unit of the Flysch Belt (r—Rača, b—Bystrica, k—Krynica nappe), 8—Internal Magura nappes of the Flysch Belt, 10—Klippen Belt,

12—Neogene sediments, 14—Andesitic volcanic rocks, 17—Inner Western Carpathian Paleogene formations, 19—Tatricum unit: a—crystalline basement, b—cover units (mostly Mesozoic), 20—Veporicum unit: a—crystalline complexes, b—cover units (Upper Paleozoic—Mesozoic), 21—Hronicum unit

and Inner (IWECA = Carpathia) based on the youngest Cenozoic (Neoalpine) tectonic processes.

The formation of the Carpathia block (CA) took place during the long-term orogenic processes during the Hercynian, Palealpine and Mesoalpine stages. During the Hercynian orogeny, the crust of today's CA, composed of Hercynian metamorphic complexes (mid-crustal nappes, Bezák et al. 1997) and granitoid intrusions, was formed. After isostatic levelling and denudation mostly in the Permian, a sedimentary Mesozoic cover sedimented on them. During the Palealpine collision (Cretaceous), basic crustal tectonic units of the CA (Tatricum, Veporicum, Gemericum) and superficial nappe systems (Fatricum, Hronicum, Meliaticum, Turnaicum, Silicicum) were formed. From the Mesoalpine

period of the collision between the Palealpine Carpathian block (with Tatricum on the head) and the PC terrane (late Cretaceous—early Paleogene), only a few fragments are preserved, the most prominent of which is the narrow tectonic KB zone along the northern edge of the Tatricum.

However, the current form of Western Carpathians, their structure and basic tectonic division are mainly the result of the last Neoalpine tectonic processes that took place from the end of the Paleogene, during the Neogene to the present. This topic is addressed by several authors (e.g. Csontos et al. 1992; Konečný et al. 2002; Schmid et al. 2008; Kováč et al. 1998; Froitzheim et al. 2008). The key process in the tectonic development of the Carpathian-Pannonian region was subduction, followed by a sublithospheric mantle rise.

This was followed by the escape of lithospheric blocks (terraces) as CA, Pelsonia, and others from the Alps into the North Penninic Ocean and their collision with the edge of the European Platform (Royden and Horváth 1988; Ratschbacher et al. 1991a,b; Horváth 1993; Linzer 1996; Kováč 2000). These processes spread from west to east and southeast. The continental collision began in the westernmost part of the Western Carpathians, later shifted to northeast, then turned southeast in the Eastern Carpathians, and finally to the south in the Southern Carpathians. The accompanying volcanism also migrated in the same way (e.g. Kováč 2000; Konečný et al. 2002; Seghedi et al. 2004).

The development in WECA also takes place in this context. In the Nealpine period, the CA moved northwards towards the stable European platform, thus closing the sea area of North Penninicum in which masses of sand and clay (flysch sediments) were sedimented since the Cretaceous, and especially during the Paleogene. Subduction of the North Penninic crust took place together with most flysch sediments. The gradual closure of the outer flysch basin from the southwest to the northeast in the Upper Eocene to Lower Miocene caused the folding of flysch sediments and their thrusting to the edge of the European Platform (e.g. Oszczyk and Zuber 2002). This way a massive strip of flysch belt was created, representing OWECA. At that time, the layers of sediments of a similar type were also deposited in the epicontinental conditions on the CA block (Inner Carpathian Paleogene sediments).

In the Neogene, extension took place in the CA area together with the formation of an arcuate basin, which was accompanied by the ascent of mantle masses (Konečný et al. 2002; Šefara et al. 1996) and subsequent volcanic processes. The emergence of horst and graben structures also occurred in this period in the CA.

The study area straddles northeastern Slovakia and southeastern Poland (Figs. 1 and 2) and comprises the northeastern part of the CA and OWECA. The OWECA represent the Cenozoic accretionary complex, known as the Flysch Belt, which overrides the down-bended European plate (e.g. Pícha et al. 2006; Ślaczka et al. 2006). The Flysch Belt consists of Late Cretaceous to Miocene deep marine clastics detached from the subducting attenuated continental or oceanic crust of the North Penninic realm (Pícha et al. 2006; Ślaczka et al. 2006; Kováč et al. 2016). In the eastern part, the Flysch Belt consists of the Magura, Dukla/Fore-Magura, and the Silesian-Krosno nappe groups (Ślaczka et al. 2006). The Magura nappe lies in the highest structural position and involves from top to bottom and from south to north the Krynica, Bystrica, and Rača units (e.g. Kováčik et al. 2011, 2012). The Dukla/Fore-Magura group of nappes involves the transitional Grybow Unit and Dukla Unit (Ślaczka et al. 2006). The Grybow Unit crops out only as tectonic windows from below the Magura nappe (Ślaczka et al. 2006; Kováčik

et al. 2011). The more external Silesian-Krosno group of nappes comprises the Silesian, Sub-Silesian, and Skole units from top to bottom and from south to north (Ślaczka et al. 2006). The cumulative thickness of the OWECA accretionary wedge reaches its maximum of about 10 km in its southern part (see e.g. Gałała et al. 2012).

The northernmost unit of CA represents a very narrow, long, and extremely complicated tectonic Klippen Belt (KB) zone (e.g. Plašienka 2018). The KB involves mostly Oravic units, which consist of Jurassic to Palaeogene sedimentary complexes detached from their basement (Pieninic crust). The Oravic units were derived from an independent palaeogeographic zone, considered an intra-oceanic ribbon continent, known as the Czorsztyn Ridge (Birkenmajer 1986) or later Oravic crust (Bezák et al. 2011) or later Penninic crust (e.g. Hrubcová et al. 2010). This ridge, which can be correlated with the Middle Penninic units of the Western Alps (Schmid et al. 2008), was separated by two branches of the Alpine Tethys from the European plate to the north and from the IWECA domain to the south (Plašienka 2018). The KB experienced complex polyphase structural deformation including Palaeocene to Eocene nappe thrusting (see e.g. Jurewicz 2005; 2018; Plašienka and Mikuš 2010; Plašienka 2012) followed by Miocene wrench tectonics, which obliterated original fold-and-thrust structures resulting in its spectacular “klippen” structure (e.g. Ratschbacher et al. 1993; Kováč and Hók 1996; Plašienka et al. 2020). Although ophiolites do not occur in the KB structure, due to its complicated structure and inferred extreme shortening, Carpathian geologists consider it as a Mesoalpine suture zone (Plašienka 2018).

The IWECA consist of a Cretaceous thrust stack involving thick- and thin-skinned thrust sheets (e.g. Plašienka 2018; Froitzheim et al. 2008). From bottom to top and from north to south they involve the Tatric basement–cover sheet overlain by the thin-skinned Fatric and Hronic cover nappes, the Veporic crustal-scale thrust wedge, and Gemeric basement–cover nappe in the SE. These units are in the study area completely covered by overstep sequences of the Inner Carpathian Paleogene Basin (Gross et al. 1999). The only place where the IWECA units outcrop is in the Branisko Mts. (Fig. 2), which, especially its northern part, is a typical fault-bounded horst structure uplifted during Miocene (Danišík et al. 2012).

The Branisko Mts. is built up mostly of Veporic, originally considered as Tatric, Hercynian crystalline basement and its Late Paleozoic to Mesozoic cover (Polák et al. 1996; Gross et al. 1999). The crystalline basement in the northern part (the Smrekovica massif), known as the Patria complex, consists of granitoids and medium to high-grade metamorphic rocks, mostly gneisses, amphibolites, and migmatites (Vozárová 1993; Faryad et al. 2005). Permian represents their sedimentary cover to Lower Triassic

siliciclastic formations reaching up to 200–400 m. The overriding Hronic nappe involves Late Paleozoic to Lower Triassic clastic formations and Middle to Upper Triassic carbonates outcropping mainly in the northern periphery of the Branisko Mts.

The southern part of the Branisko Mts., the Sľubica masif, is formed by high-grade and partly retrograde metamorphic rocks of Miklušovce and Lodina complex. Their cover consists of Late Paleozoic clastic formations and Triassic to Jurassic sedimentary succession. These formations are in places overridden by Late Paleozoic rocks assigned to the Hronic nappe (Polák et al. 1996). To the south the Veporic Unit is overridden by Late Paleozoic low-grade sedimentary complexes of the Gemer Unit along the thrust fault zone called the Lubeník(-Margecany) Line (Plašienka 2018).

The post-orogenic ICP units, representing an overstepping complex that seals all the pre-Bartonian structures in the CA, formed as a forearc basin system developed in the upper plate position behind the OWECA accretionary wedge (e.g. Soták et al. 2001; Plašienka and Soták 2015; Kováč et al. 2016). It represents the largest accommodation space for submarine fan deposits. The basin is filled by several hundred up to thousands of metres thick Bartonian to Oligocene/lowermost Miocene flysch-like deposits (Soták et al. 2001). The greatest thickness of the flysch sediments occurs in the tectonically disturbed Šambron Zone, which is about 5 km wide antiformal structure situated near the junction with the KB (Plašienka et al. 1998; Soták et al. 2001).

Profile SA-01 is located in the northeastern part of Slovakia in the Šariš region, and extends across the border into Poland (Fig. 2). The profile has a southwest-northeast orientation. Starting in the southwest in the Levočské vrchy Mts. and continues through the Paleogene sediments. The profile crosses the Klippen Belt towards the northeast and passes through the Čergov Mts. to Nízke Beskydy Mts., consisting of Outer Carpathian flysch sediments. Continuing through the flysch zone, the profile proceeds into polish Beskid Sadecky Mts (Fig. 2).

## Methods

The magnetotelluric (MT) method (Tikhonov 1950) uses a natural time-varying harmonic magnetic as a primary field to induce electromagnetic responses in conductive Earth. Maximum depth information for each period is estimated by the skin (penetration) depth and is higher with longer periods and higher resistivity of the structures (see chapter 2D inversion modelling of MT data). The range of periods is from  $10^{-4}$  s to tens of thousands of seconds. The method is well suited for imaging structures with high conductive contrast, e.g. fluids, sedimentary basins, faults, contact zones, or some mineral deposits.

The profiles SA-01 and MT-05 orientation are approximately perpendicular to the structures of the contact zone between the Inner and Outer Western Carpathians. A total of 21 sites were measured along the profile SA-01, with the majority of them installed on the Slovak side and measured by mix of Metronix company equipment and equipment from Phoenix company, while 5 were located in Poland and measured by using only equipment from Phoenix ones. The profile length is nearly 60 kms, with an intersite spacing mostly from 2 to 3 kms. In certain areas, the spacing is extended up to 7 kms, depending on the distance from sources of artificial noise. Profile MT-05 consists of 15 sites collected almost two decades ago in a frame of the MT CELEBRATION 2000 project. It is parallel to SA-01 and situated more to the south-east of the new profile. The old MT data from profile MT-05 were collected with remote reference technique by MT-1 instruments from Electromagnetic Instruments Incorporation (EMI) by PBG Warszawa Poland for ENIVIGEO Ltd. Slovakia along CELEBRATION profile 5. Parallel time series of magnetic components and 4 sets of electric components (4 times  $E_x$  and  $E_y$  spread in L configuration on the area 100 x 400 m) were processed with standard MTR15, COMBINE9, TSDEC94 processing codes.

The newly collected magnetotelluric data contains information from two horizontal electric components and two horizontal magnetic components, where each electric and magnetic component is mutually perpendicular. However, due to equipment limitations, the vertical component of the magnetic field was not recorded.

## Data analysis and processing

Before starting the inverse modelling process, preparing and analysing the data is important. Firstly, the measured time series of the varying electromagnetic fields from profile SA-01 were processed into impedance transfer functions. To perform this process, robust statistical processing methods from Metronix company (Friedrichs 2021) and Smirnov and Egbert (2012) were used. The processing of data collected with the Phoenix apparatus was performed using the robust method in the Empower software (Phoenix Geophysics Ltd.). To improve the signal-to-noise ratio of the data, we applied the remote reference technique to each of the datasets measured simultaneously (Gamble et al. 1979; Goubau et al. 1984).

The resulting impedance transfer functions were graphically plotted to illustrate how apparent resistivity and impedance phases vary with periods. To eliminate data outliers, robust Smirnov (2003) methods were employed to smooth sounding curves. The data were significantly affected by noise, mainly in the southeastern part of the profile. For this reason, valuable information could only be obtained from the periods between 1 and 10 s, which corresponds

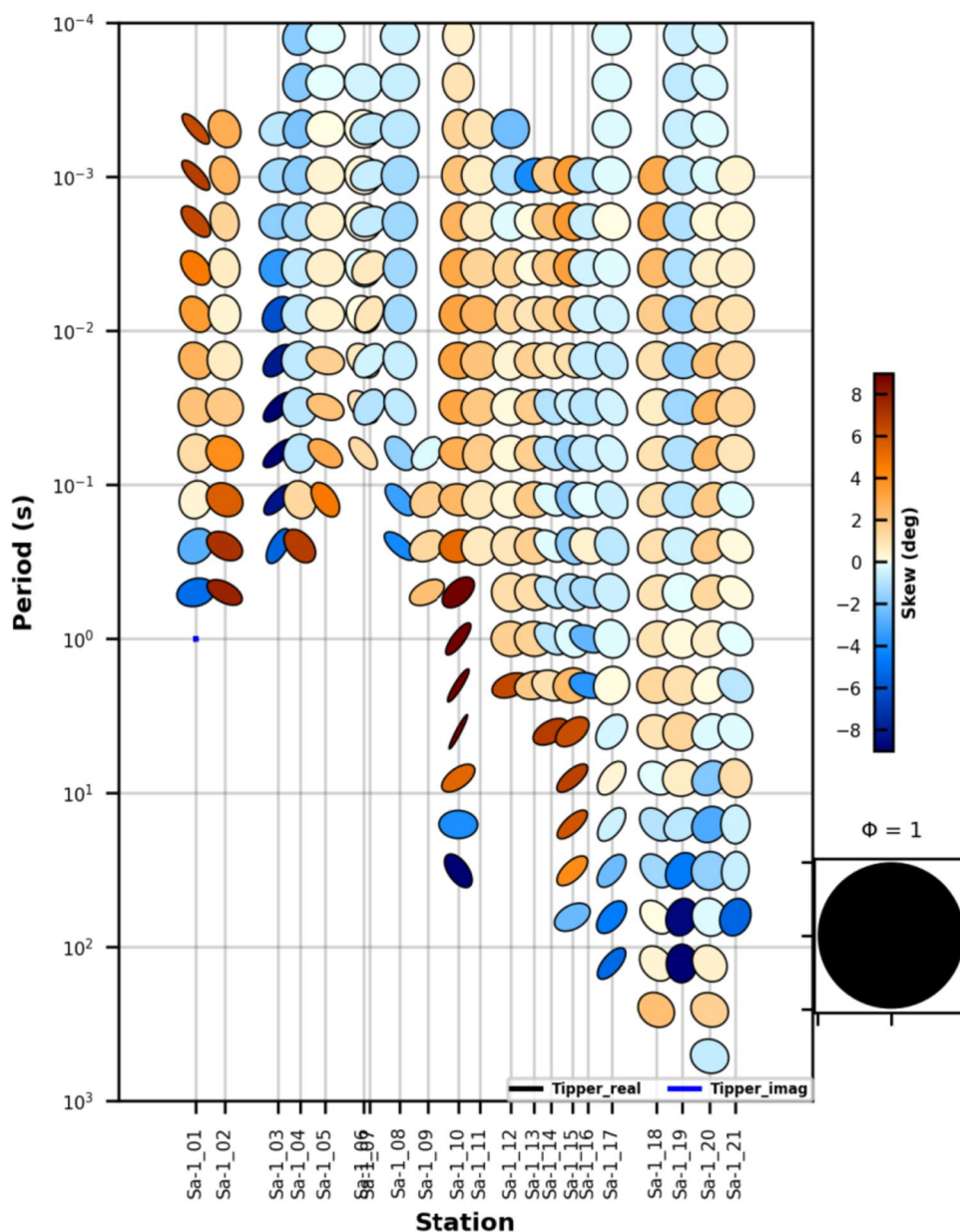
to approximately 5–15 kms in depth. However, this depth is sufficient for studying the tectonic structure of the area.

The data analysis involves determining the dimensionality and orientation of the geoelectrical structures. The dimensionality of the structures is estimated using the phase tensor (Caldwell et al. 2004), which provides information about the impedance phases. A circular shape of the tensor represents 1D data, while an elliptical shape indicates a 2D or 3D character of the data. The beta angle, which represents the deviation from the major axis of the ellipse, determines whether the data is 2D or 3D. If the beta angle is less than  $3^\circ$ , the data is considered 2D; if it is greater than  $3^\circ$ , the data is considered 3D (Caldwell et al. 2004; Kirkby 2021). The major axis of the ellipse also indicates the direction of the geoelectrical

structures, which are characterised by anomalous conductivity compared to the surrounding environment (Fig. 3). The dimensional analysis was performed using the Python toolbox MTpy (Krieger and Peacock 2014), and it revealed a predominance of 2D data character. We preferred the 2D modelling over a 3D approach due to expected significantly 2D geological situation and potential 3D structures are taken as higher dimensional noise that should be filtered out.

The orientation of the structures is determined through directional analyses, which involve finding the strike angle. To minimise distortion errors that could affect the data, a data decomposition method based on Groom and Bailey (1989) was employed.

**Fig. 3** Phase tensors of whole signal period range at each site of the profile SA-01



McNeice's and Jones's (2001) strike code was used to calculate the strike angle for all sites and all periods. The found strike angle has a value of  $-44.8^\circ$ , while a positive value of  $135.2^\circ$  was employed, representing a rotation of  $+180^\circ$  from the original value. However, this rotation indicates the same orientation of the structures for structures up to depth 10 km. Consequently, all the data were decomposed in this direction. A similar technique was used for MT data from the profile MT-05, where the period range after editing out of noisy data was from approximately 0.01–700 s. The data quality deteriorating to the southwest end of the profile. The final strike direction was estimated to be  $103^\circ$  for depth down to 30 km estimated by Niblett–Bostic transform.

## 2D inversion modelling of MT data

The processed data were imported into WinGLink software. Sounding curves of apparent resistivity and impedance phases were edited to mask outliers or any other bad data points. Due to the high noise level for longer periods, sounding curves were shortened in the southeastern part of the profile, thereby reducing the signal's frequency range. The edited sounding curves are entered into the inverse modelling process and used as input for the inverse modelling process to calculate 1D and 2D models. 1D models calculated using the Occam code (Constable et al. 1987) represent only vertical changes in the resistivity of the medium at each site, whilst 2D models provide information about the resistivity distribution in a half-space. For the calculation of 2D models, WinGLink software uses the inversion code developed by Rodi and Mackie (2001).

In 2D model approximation, electromagnetic waves propagate in two modes: transverse electric (TE) and transverse magnetic (TM), each containing different electromagnetic field components. These two modes are mutually perpendicular. In the TE mode, currents flow along 2D structures, whereas in the TM mode, currents flow perpendicular to these structures. The data of both modes can be inverted together or separately. To optimise the 2D model calculation results, both modes' apparent resistivities and impedance phases are gradually added during the calculation process.

At first, the impedance phases are inverted, because they are not affected by distortion errors of static shift. Inversion starts with only impedance phases of TE mode. Then TM mode phases are joined. Subsequently, the apparent resistivities of the TE mode and TM mode enter the inversion. Starting the inversion process with the parameters least affected by distortion generally results in better data fit.

The edited sounding curves, entered into 2D modelling, represent electromagnetic signals within a frequency range from 10 kHz up to 0.001 Hz. Based on this information the magnetotelluric method's expected penetration depth ( $h_T$ ) can be calculated using the formula:  $h_T \approx 500 \sqrt{T \rho_a}$  [m]. The

penetration depth depends on the given period (T) and the apparent resistivity of the uniform half-space ( $\rho_a$ ), typically set at 100  $\Omega\text{m}$ . Starting from the uniform half-space, the algorithm first calculates the forward solution of the discretised 2D model using a finite difference numerical method. Subsequently, an inverse model is obtained through a gradual iterative process, by calculating Nonlinear Conjugate Gradients. The size of the entire model was set to be several times larger than the profile area to ensure the stability of the numerical solution.

During the decomposition process, the data errors are replaced with smaller errors, which are then entered into the modelling as part of the data. However, it is important to set the parameters of the error floor. It represents the lowest acceptable values of errors entering into the calculation. The inverse algorithm thus assigns larger weights to lower errors, leading to a decrease in data fit and thereby increase in RMS. The error floor is usually set to 5% for impedance phases and 10% for apparent resistivities. Although impedance phases are less affected by errors, therefore their error floor is set to a lower value than the error floor for apparent resistivities. In the case of the 2D model of the SA-01 profile, the error floor values were set at 5% for impedance phases and 20% for apparent resistivities. Furthermore, the inversion code can also eliminate the distortion errors caused by static shift, resulting in apparent resistivity curves being shifted to higher and lower values. This distortion is primarily caused by small-scale inhomogeneities with anomalous contrasts to the surrounding area, occurring at shallow depths (Figs. 4 and 5). The quality of the inverse model depends on the data fit quality. Data fit is calculated as normalised residuals between the modelled and observed data through RMS (root mean square) error. A final RMS value is calculated as the average of the RMS values for each site. An ideal RMS value for the final geoelectrical model should be in the range between 1 and 2, depending on the data quality. However, if data quality is lower, an RMS value of up to 3 is still acceptable for final model interpretation. The RMS for the final inverse model of the SA-01 profile was 2.7 (detailed info about datafit in supplementary part), which could be attributed to the lower data quality in the southwestern part of the profile.

The inverse algorithm uses regularisation to balance model fitness and smoothness through the regularisation operator  $\tau$ . An ideal value for the parameter  $\tau$  could be determined by plotting the L-curve, which displays the relationship between the RMS and the roughness of the model. The ideal value of  $\tau$  is found at the greatest bend of the curve. Beyond this point, the data fit only slowly improves, and that is not sufficient to continue with further minimising the  $\tau$  value at the cost of the decreasing smoothness of the model. Too low values of  $\tau$  could create unrealistic artefacts

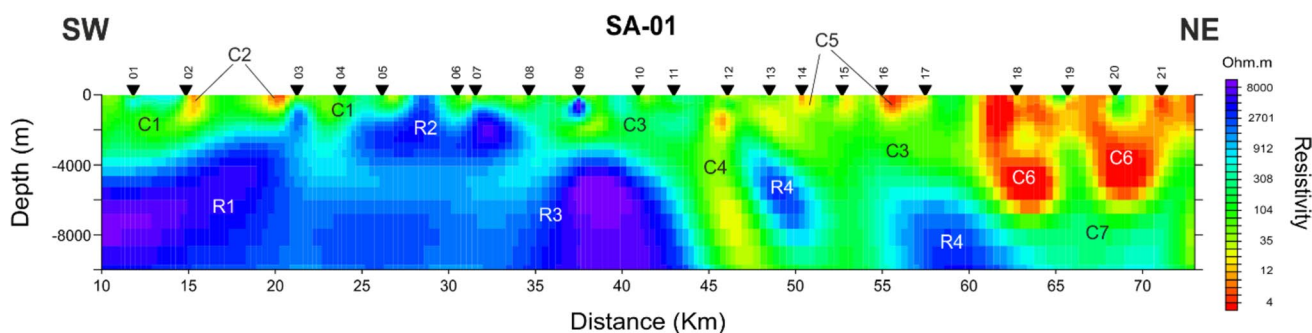


**Fig. 4** 2D MT model along SA-01 profile with higher conductivity (C1—C7) and resistive (R1-R4) structures. Black triangles show position of measured MT sites

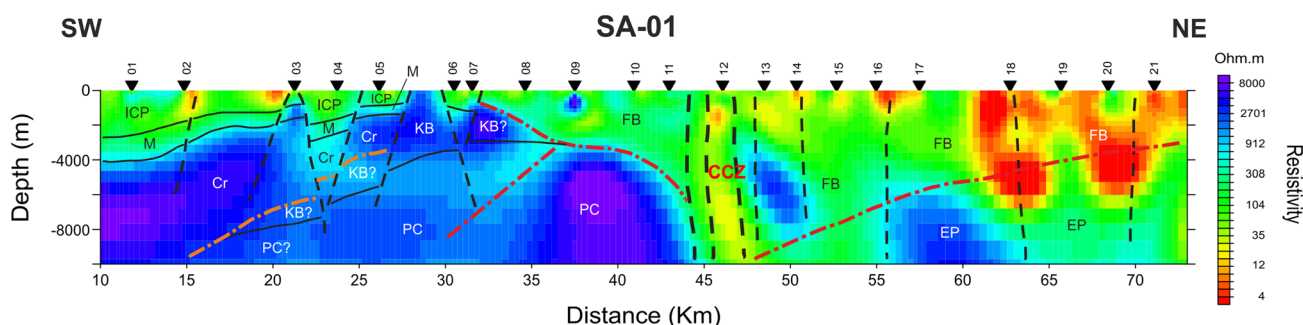


**Fig. 5** Geological interpretation of the MT profile SA-01. Explanations: ICP—Inner Carpathian Paleogene sediments, M—Mesozoic complexes, Cr—crystalline complexes of IWECA, KB—Klippen Belt, PC—Penninic crust, FB—Flysch Belt, EP—European platform, CCZ—Carpathian conductive zone. Dashed lines—presumed faults,

thick dashed—CCZ, red dot-dashed lines—structures of Neolpine collision stage (mainly thrust of flysch units on EP and their back thrust, after seismic profile CEL-05), orange dot-dashed lines—relics of Mesoalpine (Cretaceous) collision structures

in conductivity distribution. For the profile SA-01, the value of  $\tau$  was gradually reduced from 2 to 0.1.

Profile MT-05 was run with the same error floors, with static shift correction and regularisation parameter was set to 1. The final normalised RMS for data quality fit was 2.6. Due to strong noise in the southwestern area, for the four last sites (12–15) only short periods were used with low penetration and we marked the deeper area in the profile as a zone with no resolution (Fig. 6).

## 2D modelling results

The final model with a depth of more than 8 km, is shown in Fig. 4. It was selected from several models that were calculated using different inversion parameters settings. In the southwestern part of the profile, at sites 01–05, structures with a medium conductivity occur in the depth range from the surface to almost 4 km, whereas the depth of the lower boundary decreases from 4 km in southwest to 1.5 km in northeast (C1). Within this area, some small conductive near-surface structures are present (C2). They are situated directly beneath the measured sites, therefore the strongest

signal is measured there. A small near-surface resistive structure between the first and the second site of the profile could represent a small local inhomogeneity or possibly an artefact due to its shallow depth. Below this higher-conductive area in the southwestern part of the profile lying a large resistive structure, extending between the sites 05 and 06 (R2). The resistive structure continues beneath another shallow conductive area (C3) with small artefacts from site 06 to site 11. A boundary between the large resistive structure (R3) and the overlying conductive area (C3) is in increasing depth of approximately from 2 to 5 km. Below the site 12, a deep vertical conductive structure (C4) was found, which likely extends to a depth beyond the profile area. The area between sites 13 and 17 is characterised by medium conductivities (C3) with stronger conductive artefacts in shallow depths (C5). Relatively high conductive structures are situated at depths of approximately 4 km. Under sites 13 and 14, an isolated resistive structure (R4) is located within the depth range of 4–8 km. In addition, under sites 16 and 17, a relatively large resistive structure (R4) is found in depth from approximately 5.5–10 km, with a slight northwest–southeastern inclination. The northeastern part of the



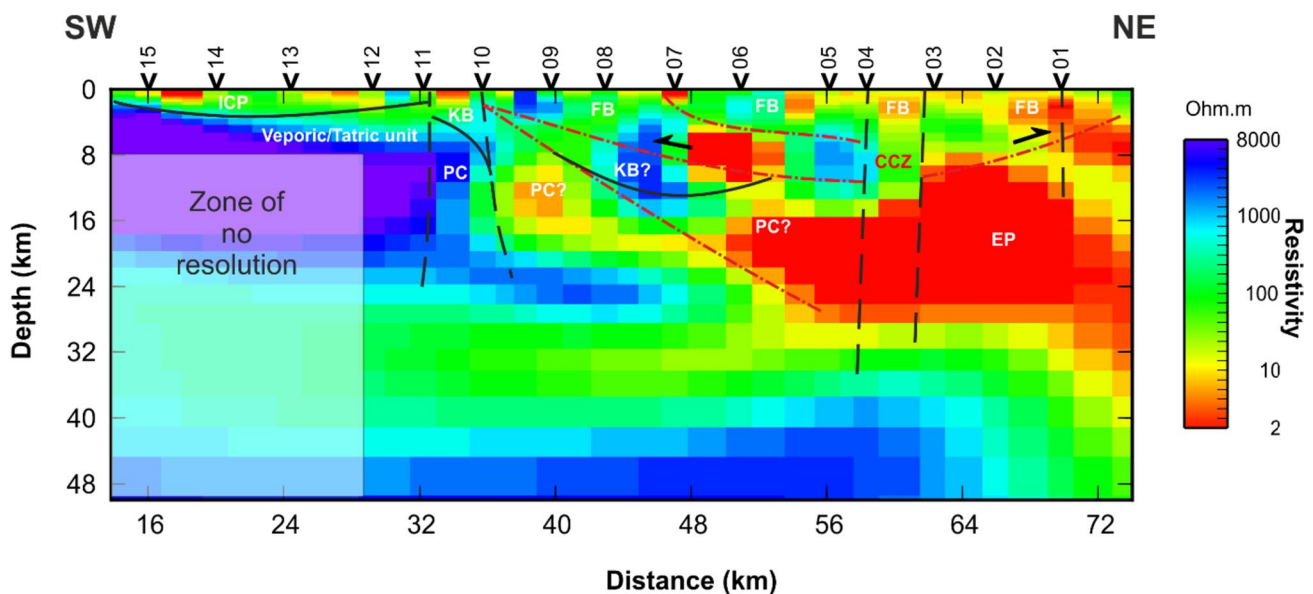


**Fig. 6** Deep MT profile MT-05. Explanations as in Fig. 5. Red lines—representation of probable structures from collision and back thrusting processes

profile in Poland is represented by medium conductivities (C7) at the bottom of the profile area with a relatively deep high conductive structures (C6) extending from a surface to a depth of 6.5 km.

### Geological interpretation

The moderately conductive structure C1 represents the sediments of the ICP and underlying Mesozoic complexes. The locally shallow conductive structures C2 are likely caused by more water-saturated sediments, probably in the vicinity of smaller faults or inversion numerical artefacts. In the basement there is a resistive complex built by crystalline rocks (R1) of Veporic or Tatric units. Another resistive structure between sites 5 and 6 (R2) belongs to the KB and deeper to the original basement of the KB–Penninic crust (R3). We assume that these complexes reach both to the south under the Veporic or Tatric complexes and to the north under the back thrustured outer flysch units (conductive structure C3). The most striking is the relatively wide steep conductive structure around site 12–13, which positionally corresponds to the course of CCZ (Fig. 1 and 2). North of it, there are only flysch nappes and the basement EP. The overall conductivity structure of this part is very irregular: it is mostly moderately conductive but contains several anomalies—both resistive (R4) and highly conductive (C6). In the previous MT models west of this area (e.g. Majcin et al. 2014), the flysch regularly maintained medium conductive properties and the EP was highly resistive. The disruption of such a structure in the studied area is caused by breaking of the entire segment away from the CCZ to the north

by the effects of fault tectonics, especially in the final trans-tensional development stage. This caused the segmentation of the foundation and the outflow of fluids and transfer of heat from greater depths (Majcin et al. 2014). It also erased the interface between the FB and EP. The relatively shallow (up to 1 km deep) conductive structures in the flysch again represent more waterlogged parts, possibly near local faults.

From the point of view of the MT model, the profile is divided into two parts by a deep sub-vertical conductive zone in the vicinity of 12–13, which coincides with the assumed course of CCZ and CCA in the map at depth (Figs. 1 and 2). For added context, the CCA is a deep conductive anomaly, which is defined by various authors at a depth of 10–25 km (Buryanov et al. 1987; Červ et al. 2001), and occurs on the northern edge of the Carpathians all around their circumference. It is assumed to be caused by hydrothermal fluids, graphite, mineralization, and others (e.g. Hvoždara and Vozár, 2004). In our previous interpretation (e.g. Bezák et al. 2015, 2021) we considered a deep tectonic structure that formed at the contact of the EP and the CA in later stages of development and became a channel for the outflow of fluids and heat from the mantle. This tectonic zone (we called it CCZ) was filled with fluids, which brought metallic elements, water and CO<sub>2</sub> (probably reduced to carbon), which became the source of CCA. CCZ is clearly visible in profile SA-01 (Fig. 5), and it is probably quite wide.

CA is located to the south of CCZ and is composed of two levels—the more conductive flysch sediments and the resistive basement. The flysch sediments belong both to the ICP and to the back thrustured units of the OWECA. They are separated by a steep KB structure between sites 08 and 09.

The KB units are also likely to be found to the north below FB and south where they rest on their original basement (PC). The Tatricum/Veporicum crystalline basement (Cr) with its Mesozoic cover and nappes units is thrust on the PC and KB from the south. Figure 5 shows the hypothetical distribution of tectonic units in the segment southwest and northeast of KB based on the known tectonic findings. The basement configuration is disrupted by the faults in the individual partial slabs.

The CCZ formed after the end of subduction-collisional processes in the space where the subducting lower plate broke off in the end. Subsequently, a transtensional process occurred by pulling the subduction from the Eastern Carpathians (Fig. 7). North of the CCZ lies a basement of the EP on which the flysch nappes were over thrust. On previous MT models in the western part of the WECA, there is a conductive contrast between the EP and FB. This contrast is probably obscured by the output of fluids and heat throughout the crust. Therefore, in the interpretation of these structures, we rely on the seismic section CEL-05 (Janik et al. 2011), of which the MT-05 section is also a part. Our MT models confirm the seismic model including the uplift of the basement in the KB area. Reflective bonds along the FB thrust testify to the original subduction and collisional structures, which are no longer visible in the MT model due to thermal reworking.

Some structures in the SA-01 profile, especially the extremely conductive ones like C6 (Fig. 4), would be very

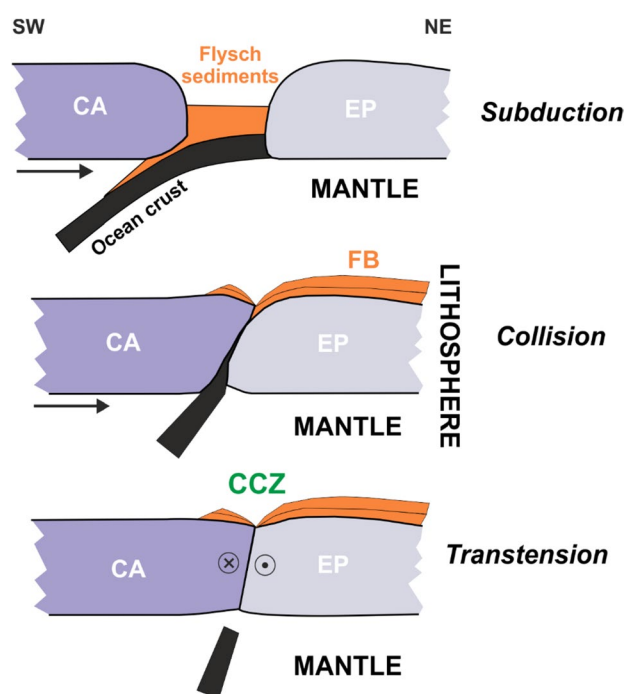


**Fig. 7** Imagination of tectonic evolution of the contact between CA and EP during Neopalpine stage on the base of MT models

difficult to explain without the support of MT modelling along the MT-05 profile (Fig. 6), which stretches along the profile SA-01 in its close vicinity. In profile MT-05, the conductive structures in the middle crust at a depth of 8–24 km are prominent. They probably follow the tectonic structures that emerged during the collision processes at the end of subduction. These structures, or weakened tectonic zones, were a channel for the outflow of fluids from the mantle. At a later stage—during the formation of the CCZ, which was also in contact with the mantle—they were yet again saturated with fluids and in the vicinity also by the penetration of volcanic masses (Kucharič et al. 2013) and the output of heat flow (Majcin et al. 2014).

Due to the fact that there are locally missing low-frequency data, geological details are lost in the deep MT-05 profile (Fig. 6), but large crustal structures become more prominent. The most striking are the wide conductive zones, which are mainly located in the middle crust. That structure corresponds well to the recently calculated deep resistivity model for the whole of Poland (Józwiak et al. 2022). These structures have no counterparts in other profiles in Central (profile MT 2 T, Vozár et al. 2021) or Western (MT-15, Bezák et al. 2015) Slovakia, except for the southern part of the 2 T profile, where they have been interpreted as the young reworking of the crust by volcanic or hydrothermal fluids (Bezák et al. 2015).

Large conductive zones in the crust are genetically young and we associate them with the Neopalpine tectonic processes in the Neogene. These include the subduction of flysch complexes and parts of their basement, followed by processes of advancing subduction to the east associated with extension, intrusions of mantle material and fluids into the crust, and volcanism. All tectonic structures were used by the output of fluids, which caused the formation of conductive zones. We believe that these conductive structures reflect these progressive tectonic phases, and therefore do not belong to a single event, but to a number of mutually consecutive processes. In the MT-05 profile, we can see conductive structures in the northern part, which probably arose along tectonic planes that formed during subduction and during back-arc thrusting.

## Discussion

The SA-01 MT profile completes a series of MT profiles across the contact zone between Neopalpine IWECA block and EP. Starting from the west with the MT-15 profile (Bezák et al. 2014), followed by profiles in central northern Slovakia (Bezák et al. 2021) and the SA-01 is the easternmost one (if we count only published MT profiles).

We propose to replace the term IWECA (Inner Western Carpathian) with term Carpathia for compatibility with other

terrane names in the Pannonian area. The content of the Carpathia remains the same as IWECA (Hercynian, Palealpine, and Mesoalpine units), and is outlined by blue lines in Fig. 1. An accretionary wedge of flysch OWECA was formed during the collision of CA with EP.

All previous MT models have brought new light to the interpretation of the contact between CA and EP. In the case of MT profile SA-01 and MT-05, it can be stated that they are dominated by steep tectonic zones, which are a reflection of the youngest fault tectonics. The CCZ is the most striking one of them all. The faults broke also the basement in both CA and EP, as documented before (e.g. Ryľko and Tomáš 2005). From the other structures, the back thrust of the flysch units to the south on CA is also significant. New information is the existence of important conductive zones, mainly in the middle crust, which probably copies previous collisional and next transtensional structures. We propose that their source is asthenolitic masses from the mantle.

Generally accepted tectonic models for contact of CA and EP is the existence of subduction and subsequent collision processes, which is also evidenced by the KB and FB structures in a wider area (e.g. Jurewicz 2018; Plašienka et al. 2020; Majcin et al. 2018). The overthrust of FB on EP is documented together with the overthrust of KB on FB. In other parts of the orogen, the back thrust of the FB to the CA is also preserved (Birkenmajer 1986; Plašienka et al. 2013). The seismic sections of this area also confirm such a constellation (Grad et al. 2006; Janik et al. 2011). According to the results of MT modelling, the subduction-collision structure of this area was destroyed by younger steep faults, but mainly by the output of fluids and heat, which changed the distribution of conductivity parameters of individual geological units that participate in the construction of the area.

Despite the destruction of older structures, signs of previous development remained in the SA-01 and MT-05 MT sections. Thus, the mid-crustal channels of conductive structures captured mainly in the MT-05 model, carried out during subduction, testify in favour of the subduction processes. The back thrust structure of flysch units, which is visible in both MT and seismic models, is a manifestation of the collision processes.

## Conclusion

The MT sections SA-01 and MT-05, measured in NE Slovakia and SE Poland, were oriented across the contact zone between CA and EP. These MT sections yielded additional data on the structures formed by the interaction between these tectonic blocks. First, the CCZ structure dominates in this area. We interpret it as a sub-vertical tectonic zone that separates resistive blocks CA and EP. It emerged after the disappearance in the subduction zone between them and

after the subsequent collision, which turned into transpressional and later transtensional movements.

Traces of subduction were not preserved in the MT image, but they are visible in seismic results. The MT-05 profile was measured along part of the CEL-05 seismic profile, so their comparison is easy and the structures in both models are very similar. The structures that accompanied subduction were used in the output of hydrothermal fluids or volcanic material from the mantle. These significantly affected the conductive properties of the crust in this area, and are manifested as wide conductive mid-crustal zones parallel to the former subduction and back thrust structures. The fluid outputs also continued in the subsequent mode, with CCZ functioning as the supply channel. The fluids and volcanics were also the carriers of heat, they increased the heat flow in the area and changed the original conductivity parameters of the basement complexes.

**Supplementary Information** The online version contains supplementary material available at <https://doi.org/10.1007/s11600-023-01239-6>.

**Acknowledgements** This work was supported by the Slovak Research and Development Agency under the Contract no. APVV-21-0159, APVV-16-0482 and VEGA project 2/0171/24. We thank RNDr. Alexandra Marsenić, PhD. and Andrej Bezák for their help with the field work.

## Declarations

**Conflict of interest** The authors have no relevant financial or non-financial interests to disclose.

**Open Access** This article is licensed under a Creative Commons Attribution 4.0 International License, which permits use, sharing, adaptation, distribution and reproduction in any medium or format, as long as you give appropriate credit to the original author(s) and the source, provide a link to the Creative Commons licence, and indicate if changes were made. The images or other third party material in this article are included in the article's Creative Commons licence, unless indicated otherwise in a credit line to the material. If material is not included in the article's Creative Commons licence and your intended use is not permitted by statutory regulation or exceeds the permitted use, you will need to obtain permission directly from the copyright holder. To view a copy of this licence, visit <http://creativecommons.org/licenses/by/4.0/>.

## References

- Bezák V, Jacko S, Janák M, Lederer P, Petřík I, Vozárová A (1997) Main Hercynian lithotectonic units of the Western Carpathians. *Mineralia Slovaca-Monographs. Geological evolution of the Western Carpathians (Mineralia Slovaca Monograph)*. Geocomplex, Bratislava, pp 261–269
- Bezák V, Pek J, Vozár J, Bielik M, Vozár J (2014) Geoelectrical and geological structure of the crust in Western Slovakia. *Stud Geophys Geod* 58(3):473–488. <https://doi.org/10.1007/s11200-013-0491-9>
- Bezák V, Pek J, Majcin D, Bučová J, Šoltis T, Bilčík D, Klanica R (2015) Geological interpretation of magnetotelluric sounding

- in the southern part of seismic profile 2T (Central Slovakia). *Contrib Geophys Geod* 45(1):1–11. <https://doi.org/10.1515/congeo-2015-0009>
- Bezák V, Vozár J, Majcin D, Klanica R, Madarás J (2021) Contrasting tectonic styles of the western and eastern parts of the Western Carpathian Klippen Belt based on magnetotelluric sounding of deep tectonic structures. *Geol Quart* 65(2):25
- Bezák V (ed.), Broska I, Ivanička J, Reichwalder P, Vozár J, Polák M, Havrila M, Mello J, Biely A, Plašienka D, Potfaj M, Konečný V, Lexa J, Kaličiak M, Žec B, Vass D, Elečko M, Janočko J, Pereszlényi M, Marko F, Maglay J, Pristaš J (2004) Tectonic map of Slovak Republic 1:500,000. MŽP SR, Bratislava
- Bezák V, Biely A, Elečko M, Konečný V, Mello J, Polák M, Potfaj M (2011) A new synthesis of the geological structure of Slovakia - the general geological map at 1 : 200 000 scale. *Geol Q* 55:1–8
- Birkenmajer K (1986) Stages of structural evolution of the Pieniny Klippen Belt, Carpathians. *Stud Geol Pol* 88:7–32
- Buryanov VB, Gordyenko VV, Zavgorodnyaya OV, Kulik SN, Logvinov IM, Shuman VH (1987) Geophysical model of tectonosphere of Europe. *Nauk Dumka, Kiev* (in Russian)
- Caldwell TG, Bibby HM, Brown C (2004) The magnetotelluric phase tensor. *Geophys J Int* 158(2):457–469. <https://doi.org/10.1111/j.1365-246X.2004.02281.x>
- Červ V, Kováčiková S, Pek J, Pěčová J, Praus O (2001) Geoelectrical structure across the Bohemian Massif and the transition zone to the West Carpathians. *Tectonophysics* 332(1–2):201–210. [https://doi.org/10.1016/S0040-1951\(00\)00257-2](https://doi.org/10.1016/S0040-1951(00)00257-2)
- Constable SC, Parker RL, Constable CG (1987) Occam's inversion: a practical algorithm for generating smooth models from electromagnetic sounding data. *Geophysics* 52(3):289–300. <https://doi.org/10.1190/1.1442303>
- Csontos L, Nagymarosy A, Horváth F, Kováč M (1992) Tertiary evolution of the Intra-Carpathian area: a model. *Tectonophysics* 208(1–3):221–241. [https://doi.org/10.1016/0040-1951\(92\)90346-8](https://doi.org/10.1016/0040-1951(92)90346-8)
- Danišík M, Kohút M, Evans NJ, McDonald BJ (2012) Eo-Alpine metamorphism and the mid-Miocene thermal event in the Western Carpathians (Slovakia): new evidence from multiple thermochronology. *Geol Mag* 149(1):158–171. <https://doi.org/10.1017/S0016756811000963>
- Faryad SW, Ivan P, Jacko S (2005) Metamorphic petrology of metabasites from the Branisko and Čierna Hora Mts. (Western Carpathians, Slovakia). *Geol Carpath* 56(1):3–16
- Friedrichs B (2021) ProcMT online manual, Processing code. [https://www.geo-metronix.de/metronix\\_manuals/en/pr](https://www.geo-metronix.de/metronix_manuals/en/pr). Accessed 12 Jan 2023
- Froitzheim N, Plašienka D, Schuster R (2008) Alpine tectonics of the Alps and Western Carpathians. In: McCann T (ed) *The geology of central Europe Mesozoic and Cenozoic*, vol 2. Geological Society Publishing House, London, pp 1141–1232. <https://doi.org/10.1144/CEV2P.6>
- Gągała Ł, Vergés J, Saura E, Malata T, Ringenbach JC, Werner P, Krzywiec P (2012) Architecture and orogenic evolution of the northeastern Outer Carpathians from cross-section balancing and forward modeling. *Tectonophysics* 532–535:223–241. <https://doi.org/10.1016/j.tecto.2012.02.014>
- Gamble TD, Goubau WM, Clarke J (1979) Magnetotellurics with a remote magnetic reference. *Geophysics* 44(1):53–68. <https://doi.org/10.1190/1.1440923>
- Goubau WM, Maxton PM, Koch RH, Clarke J (1984) Noise correlation lengths in remote reference magnetotellurics. *Geophysics* 49(4):433–438. <https://doi.org/10.1190/1.1441678>
- Grad M, Guterch A, Keller GR, Janik T, Hegedűs E, Vozár J, Ślaczka A, Tiira T, Yliniemi J (2006) Lithospheric structure beneath trans-Carpathian transect from Precambrian platform to Pannonian basin: CELEBRATION 2000 seismic profile CEL05. *J Geophys Res* 111(B3):B03301. <https://doi.org/10.1029/2005JB003647>
- Groom RW, Bailey RC (1989) Decomposition of magnetotelluric impedance tensors in the presence of local three-dimensional galvanic distortion. *J Geophys Res* 94(B2):1913–1925. <https://doi.org/10.1029/JB094iB02p01913>
- Gross P (ed), Buček S, Ďurkovič T, Filo I, Karoli S, Maglay J, Nagy A, Halouzka R, Spišák Z, Žec B, Vozár J, Borza V, Lukáčik E, Mello J, Polák M, Janočko J (1999) Geological map of Popradská kotlina Basin, Hornádska kotlina Basin, Levoča Mts., Spišsko-Šarišské medzihorie Depression, Bachureň Mts. and Šarišská vrchovina Highlands 1: 50 000. MŽP SR – ŠGÚDŠ, Bratislava
- Horváth F (1993) Towards a mechanical model for the formation of the Pannonian basin. *Tectonophysics* 226:333–357. [https://doi.org/10.1016/0040-1951\(93\)90126-5](https://doi.org/10.1016/0040-1951(93)90126-5)
- Hrubcová P, Šroda P, Grad M, Geissler WH, Guterch A, Vozár J, Hegedűs E (2010) From the Variscan to the Alpine Orogeny: crustal structure of the Bohemian Massif and the Western Carpathians in the light of the SUDETES 2003 seismic data. *Geophys J Int* 183(2):611–633. <https://doi.org/10.1111/j.1365-246X.2010.04766.x>
- Hvozďara M, Vozár J (2004) Laboratory and geophysical implications for explanation of the nature of the carpathian conductivity anomaly. *Acta Geophys Pol* 52(4):497–508
- Janik T, Grad M, Guterch A, Work C (2009) Seismic structure of the lithosphere between the East European Craton and the Carpathians from the net of CELEBRATION 2000 profiles in SE Poland. *Geol Quart* 53(1):141–157
- Janik T, Grad M, Guterch A, Vozár J, Bielik M, Vozárova A, Hegedűs E, Kovács CA, Kovács I, Keller GR, CELEBRATION 2000 Working Group (2011) Crustal structure of the Western Carpathians and Pannonian Basin: Seismic models from CELEBRATION 2000 data and geological implications. *Journal of Geodynamics* 52(2):97–113. <https://doi.org/10.1016/j.jog.2010.12.002>
- Jóźwiak W, Nowożyński K, Mazur S, Jeż M (2022) Deep electrical resistivity structure of the European lithosphere in Poland derived from 3-D inversion of magnetotelluric data. *Surv Geophys* 43:1563–1586. <https://doi.org/10.1007/s10712-022-09716-1>
- Jurewicz E (2005) Geodynamic evolution of the Tatra Mts. and the Pieniny Klippen Belt (Western Carpathians): problems and comments. *Acta Geol Pol* 55(3):295–338
- Jurewicz E (2018) The Šariš Transitional Zone, revealing interactions between Pieniny Klippen Belt, Outer Carpathians and European platform. *Swiss J Geosci* 111(1–2):245–267. <https://doi.org/10.1007/s00015-017-0297-9>
- Kirkby A (2021) MTPy for magnetotelluric data analysis and visualisation. *Geoscience Australia–Eminar*. [https://www.mtnet.info/EMinars/20210224\\_Kirkby\\_EMinar.pdf](https://www.mtnet.info/EMinars/20210224_Kirkby_EMinar.pdf). Accessed 6 Feb 2023
- Konečný V, Kováč M, Lexa J, Šefara J (2002) Neogene evolution of the Carpatho-Pannonian region: an interplay of subduction and back-arc diapiric uprise in the mantle. *European Geosciences Union*, 2002. *Stephan Mueller Spec Publ Ser* 1:105–123
- Kováč P, Hók J (1996) Tertiary development of the western part of Klippen Belt. *Slovak Geol Mag* 2(2):137–149
- Kováč M, Nagymarosy A, Oszczytko N, Ślaczka A, Csontos L, Marunteanu M, Matenco L, Márton M (1998) Palinspastic reconstruction of the Carpathian-Pannonian region during the Miocene. In: Rákus M (ed) *Geodynamic development of the Western Carpathians*. Geological Survey of Slovak Republic, Bratislava, pp 189–217
- Kováč M, Plašienka D, Soták J, Vojtko R, Oszczytko N, Less G, Čosovič V, Fügenschuh B, Králiková S (2016) Paleogene palaeogeography and basin evolution of the Western Carpathians, Northern Pannonian domain and adjoining areas. *Global Planet Change* 140:9–27. <https://doi.org/10.1016/j.gloplacha.2016.03.007>

- Kováč M (2000) Geodynamic, palaeogeographical and structural development of the Carpathian-Pannonian region in the Miocene. Veda, Bratislava, pp 202 (in Slovak)
- Kováčik M, Bóna J, Gazdačko J, Kobulský J, Maglay J, Kučera M (2011) Geological map of Nízke Beskydy–West 1: 50 000. MŽP SR–ŠGÚDŠ, Bratislava
- Kováčik M, Bóna J, Gazdačko L, Kobulský J, Maglay J, Žecová K, Derco J, Zlinská A, †Siráňová Z, Boorová D, Bónová K, Buček S, Kucharič L, Kubeš P, Bačová N, Petro L, Vaněková H (2012) Explanations to Geological map of Nízke Beskydy–West 1: 50 000. ŠGÚDŠ, Bratislava, pp. 180
- Krieger L, Peacock JR (2014) MTpy: a python toolbox for magnetotellurics. *Comput Geosci* 72:167–175. <https://doi.org/10.1016/j.cageo.2014.07.013>
- Kucharič L, Bezák V, Kubeš P, Konečný V, Vozár J (2013) New magnetic anomalies of the outer Carpathians in NE Slovakia and their relationship to the Carpathian conductivity zone. *Geol Quart* 57(1):123–134. <https://doi.org/10.7306/gq.1079>
- Lexa J, Bezák V, Elečko M, Mello J, Polák M, Potfaj M, Vozár J (eds) (2000) Geological map of the western Carpathians and adjacent areas 1:500,000. Ministry of the Environment of Slovak Republic, Geological Survey of Slovak Republic, Bratislava
- Linzer HG (1996) Kinematics of retreating subduction along the Carpathian arc. *Rom Geol* 24(2):167–170. [https://doi.org/10.1130/0091-7613\(1996\)024%3c0167:KORSAT%3e2.3.CO;2](https://doi.org/10.1130/0091-7613(1996)024%3c0167:KORSAT%3e2.3.CO;2)
- Majcin D, Bilčík D, Kutas R, Hlavňová P, Bezák V, Kucharič L (2014) Regional and local phenomena influencing the thermal state in the flysch belt of the northeastern part of Slovakia. *Contrib Geophys Geod* 44(4):271–292. <https://doi.org/10.1515/congeo-2015-0006>
- Majcin D, Bezák V, Klanica R, Vozár J, Pek J, Bilčík D, Telecký J (2018) Klippen Belt, Flysch Belt and Inner Western Carpathian Paleogene basin relations in the Northern Slovakia by magnetotelluric imaging. *Pure Appl Geophys* 175(10):3555–3568. <https://doi.org/10.1007/s00024-018-1891-0>
- McNeice GW, Jones AG (2001) Multisite, multifrequency tensor decomposition of magnetotelluric data. *Geophysics* 66(1):158–173. <https://doi.org/10.1190/1.1444891>
- Oszczypko N, Zuber A (2002) Geological and isotopic evidence of diagenetic waters in the Polish Flysch Carpathians. *Geol Carpath* 53(4):257–268
- Picha FJ, Stráník Z, Krejčí O (2006) Geology and hydrocarbon resources of the outer Western Carpathians and their foreland, Czech Republic. In: Golonka J, Picha FJ (eds) *The Carpathians and their foreland: geology and hydrocarbon resources*, Memoir 84. American Association of Petroleum Geologists, Tulsa, pp 49–175
- Plašienka D (2012) Early stages of structural evolution of the Carpathian Klippen Belt (Slovakian Pieniny sector). *Miner Slovaca* 44:1–16
- Plašienka D (2018) Continuity and episodicity in the early Alpine tectonic evolution of the Western Carpathians: how large-scale processes are expressed by the orogenic architecture and rock record data. *Tectonics* 37(7):2029–2079. <https://doi.org/10.1029/2017TC004779>
- Plašienka D, Mikuš V (2010) Geological structure of the Pieniny and Šariš sectors of the Klippen belt between the Litmanová and Drienica villages in eastern Slovakia. *Miner Slovaca* 42(2):155–178 (in Slovak with English summary)
- Plašienka D, Soták J (2015) Evolution of late cretaceous-palaeocene synorogenic basins in the Pieniny Klippen Belt and adjacent zones (Western Carpathians Slovakia): tectonic controls over a growing orogenic wedge. *Ann Soc Geol Pol* 85(1):43–76
- Plašienka D, Soták J, Prokešová R (1998) Structural profiles across the Šambron-Kamenica Periklippen zone of the central Carpathian Paleogene Basin in NE Slovakia. *Miner Slovaca* 30:173–184
- Plašienka D, Józsa Š, Gedl P, Madzin J (2013) Fault contact of the Pieniny Klippen Belt with the Central Carpathian Paleogene Basin (Western Carpathians): new data from a unique temporary exposure in Lutina village (Eastern Slovakia). *Geol Carpath* 64(2):165–168
- Plašienka D, Bučová J, Šimonová V (2020) Variable structural styles and tectonic evolution of an ancient backstop boundary: the Pieniny Klippen Belt of the Western Carpathians. *Int J Earth Sci* 109:1355–1376. <https://doi.org/10.1007/s00531-019-01789-5>
- Polák M, Jacko S, Vozár J, Vozárová A, Gross P, Harčár J, Sasvári T, Zacharov M, Baláz B, Karoli S, Nagy A, Buček S, Maglay J, Spišák Z, Žec B, Filo I, Janočko J (1996) Geological map of the Branisko and Čierna hora Mts. 1: 50 000. MŽP SR–ŠGÚDŠ, Bratislava
- Ratschbacher L, Frisch W, Linzer HG, Merle O (1991a) Lateral extrusion in the Eastern Alps, part 2. *Struct Anal Tecton* 10(2):257–271. <https://doi.org/10.1029/90TC02623>
- Ratschbacher L, Merle O, Davy PH, Cobbold P (1991b) Lateral extrusion in the Eastern Alps, part 1. Boundary conditions and experiments scaled for gravity. *Tectonics* 10(2):245–256. <https://doi.org/10.1029/90TC02622>
- Ratschbacher L, Frisch W, Linzer HG, Sperner B, Meschede M, Decker K, Nemčok M, Nemčok J, Grygar R (1993) The Pieniny Klippen Belt in the Western Carpathians of northeastern Slovakia: structural evidence for transpression. *Tectonophysics* 226(1–4):471–483. [https://doi.org/10.1016/0040-1951\(93\)90133-5](https://doi.org/10.1016/0040-1951(93)90133-5)
- Rodi W, Mackie RL (2001) Nonlinear conjugate gradients algorithm for 2-D magnetotelluric inversion. *Geophysics* 66(1):174–187. <https://doi.org/10.1190/1.1444893>
- Royden LH, Horváth F (1988) The Pannonian basin: a study in basin evolution, Memoir 45. American Association of Petroleum Geologists, Tulsa, p 463
- Rytko W, Tomáš A (2005) Basement structure below the West-Carpathian–East-Carpathian orogeny junction (eastern Poland, north-eastern Slovakia and western Ukraine). *Geol Carpath* 56:29–40
- Schmid SM, Bernoulli D, Fügenschuh B, Matenco L, Schefer S, Schuster R, Tischler M, Ustaszewski K (2008) The alpine-Carpathian-Dinaridic orogenic system: correlation and evolution of tectonic units. *Swiss J Geosci* 101:139–183. <https://doi.org/10.1007/s00015-008-1247-3>
- Šefara J, Bielik M, Konečný P, Bezák V, Hurai V (1996) The latest stage of development of the lithosphere and its interaction with the asthenosphere (Western Carpathians). *Geol Carpath* 47:339–347
- Seghedi I, Downes H, Szakács A, Mason PRD, Thirlwall MF, Roşu E, Pácskay Z, Márton E, Panaiotu C (2004) Neogene-quaternary magmatism and geodynamics in the Carpathian-Pannonian region: a synthesis. *Lithos* 72:117–146. <https://doi.org/10.1016/j.lithos.2003.08.006>
- Ślaczka A, Kruglow S, Golonka J, Oszczypko N, Popadyuk I (2006) The general geology of the outer Carpathians, Poland, Slovakia, and Ukraine. In: Golonka J, Picha F (eds) *The Carpathians and their foreland: geology and hydrocarbon resources*, Memoir 84. American Association of Petroleum Geologists, pp 221–258
- Smirnov MY (2003) Magnetotelluric data processing with a robust statistical procedure having a high breakdown point. *Geophys J Int* 152(1):1–7. <https://doi.org/10.1046/j.1365-246X.2003.01733.x>
- Smirnov MY, Egbert GD (2012) Robust principal component analysis of electromagnetic arrays with missing data. *Geophys J Int* 190(3):1423–1438. <https://doi.org/10.1111/j.1365-246X.2012.05569.x>
- Soták J, Pereszlenyi M, Marschalko R, Milička J, Starek D (2001) Sedimentology and hydrocarbon habitat of the submarine-fan deposits of the Central Carpathian Paleogene Basin (NE Slovakia). *Mar Petrol Geol* 18(1):87–114. [https://doi.org/10.1016/S0264-8172\(00\)00047-7](https://doi.org/10.1016/S0264-8172(00)00047-7)
- Tikhonov AN (1950) On determining electrical characteristics of the deep layers of the Earth's crust. *Doklady Acad Nauk SSSR* 73(2):295–297 (in Russian)

Vozár J, Bezák V, Marko F (2021) Three-dimensional magnetotelluric model along seismic profile 2T: an improved view on crustal structure in central Slovakia (Western Carpathians). *Geol Carpath* 72(2):85–95

Vozárová A (1993) Pressure-temperature conditions of metamorphism in the northern part of the Branisko crystalline complex. *Geol Carpath* 44:219–232